Chemical Engineering Journal 417 (2021) 128028

Contents lists available at ScienceDirect

Chemical Engineering Journal

journal homepage: www.elsevier.com/locate/cej

In-situ phosphine oxide physical networks: A facile strategy to achieve durable flame retardant and antimicrobial treatments of cellulose

Rashid Nazir [a,1], Dambarudhar Parida [a,1], Joel Borgstädt [a,1], Sandro Lehner [a], Milijana Jovic [a], Daniel Rentsch [b], Ezgi Bülbül [a], Anja Huch [c], Stefanie Altenried [d], Qun Ren [d], Patrick Rupper [a], Simon Annaheim [e], Sabyasachi Gaan [a,*]

[a] Laboratory of Advanced Fibers, Empa, Swiss Federal Laboratories for Materials Science and Technology, Lerchenfeldstrasse 5, CH-9014 St. Gallen, Switzerland
[b] Laboratory for Functional Polymers, Empa, Swiss Federal Laboratories for Materials Science and Technology, Überlandstrasse 129, CH-8600 Dübendorf, Switzerland
[c] Cellulose & Wood Materials Lab, Empa, Swiss Federal Laboratories for Materials Science and Technology, Überlandstrasse 129, CH-8600 Dübendorf, Switzerland
[d] Biointerfaces, Empa Swiss Federal Laboratories for Materials Science and Technology, Lerchenfeldstrasse 5, CH-9014 St. Gallen, Switzerland
[e] Laboratory for Biomimetic Membranes and Textiles, Empa, Swiss Federal Laboratories for Materials Science and Technology, Lerchenfeldstrasse 5, CH-9014 St. Gallen, Switzerland

ARTICLE INFO

Keywords:
Flame retardant
Cellulose
Michael addition
Antimicrobial
Durable

ABSTRACT

A facile methodology to durably modify cellulose fibers by forming in-situ phosphine oxide macromolecular physical networks is developed in this work. Such networks were formed by treating the cellulose fibers with a mixture of Michael adducts [trivinyl phosphine oxide (TVPO) and cyclic amines (piperazine and 2,4,6-tri(piperazine-1-yl)-1,3,5-triazine)] followed by a click crosslinking reaction initiated by dry heat, microwave, or steaming process. The in-situ phosphine oxide network is integrated within the cellulose fibers to produce a durable treatment against laundering. NMR and SEM analysis of the treated fibers verified the in-situ formation of phosphine oxide macromolecules in the bulk of cellulose fiber. The treatment was homogenous and achieved an outstanding phosphorus (P) retention (>95%) after even 50 laundry cycles. The treated cotton exhibited excellent fire retardant properties with a limiting oxygen index value >27% and passed the Swiss vertical flammability test at 2 wt% P. Analysis of evolved gasses during thermal decomposition of treated cellulose supported both the condensed and gas phases mechanism. The flame retardant treatment was further adapted to include antimicrobial properties by in-situ formation of silver nanoparticles within the cellulose fibers using a single-step process to demonstrate the versatility of this novel treatment methodology. The treated fabric exhibited excellent antimicrobial as well as flame retardant properties and was also durable to 50 laundry cycles. Contact angle measurements and moisture management test confirmed the excellent comfort behavior of the treated cellulose fabric.

1. Introduction

There is a growing demand to develop protective textiles for emergency workers, technical, security, and military personnel, to reduce exposure to biological, chemical, and fire threats [1–3]. Increased use of polymeric materials in building construction [3,4] and climate change [5], has led to an increase in fire incidents, which has resulted in the catastrophic wildfire, civilian and deaths, injuries, and property damage. Likewise, the spread of infectious diseases has increased over the past decades, which has great social and economic impacts [6]. Thus, novel multifunctional materials that can aid in minimizing these threats are of great importance to today's society.

Textiles are considered the first line of personal defense against the above-mentioned threats [7]. To address these challenges, innovations in textile construction and material components are of paramount importance. Cellulose is the most abundant polymer globally, and cellulose-based fibers still constitute more than 30% of the world's total fiber consumption. As renewable and biodegradable materials, they are considered sustainable compared to most engineered fibers [8]. However, like most organic materials, they burn easily and require

* Corresponding author.
E-mail address: sabyasachi.gaan@empa.ch (S. Gaan).
[1] Authors contributed equally.

https://doi.org/10.1016/j.cej.2020.128028
Received 11 September 2020; Received in revised form 18 November 2020; Accepted 3 December 2020
Available online 9 December 2020

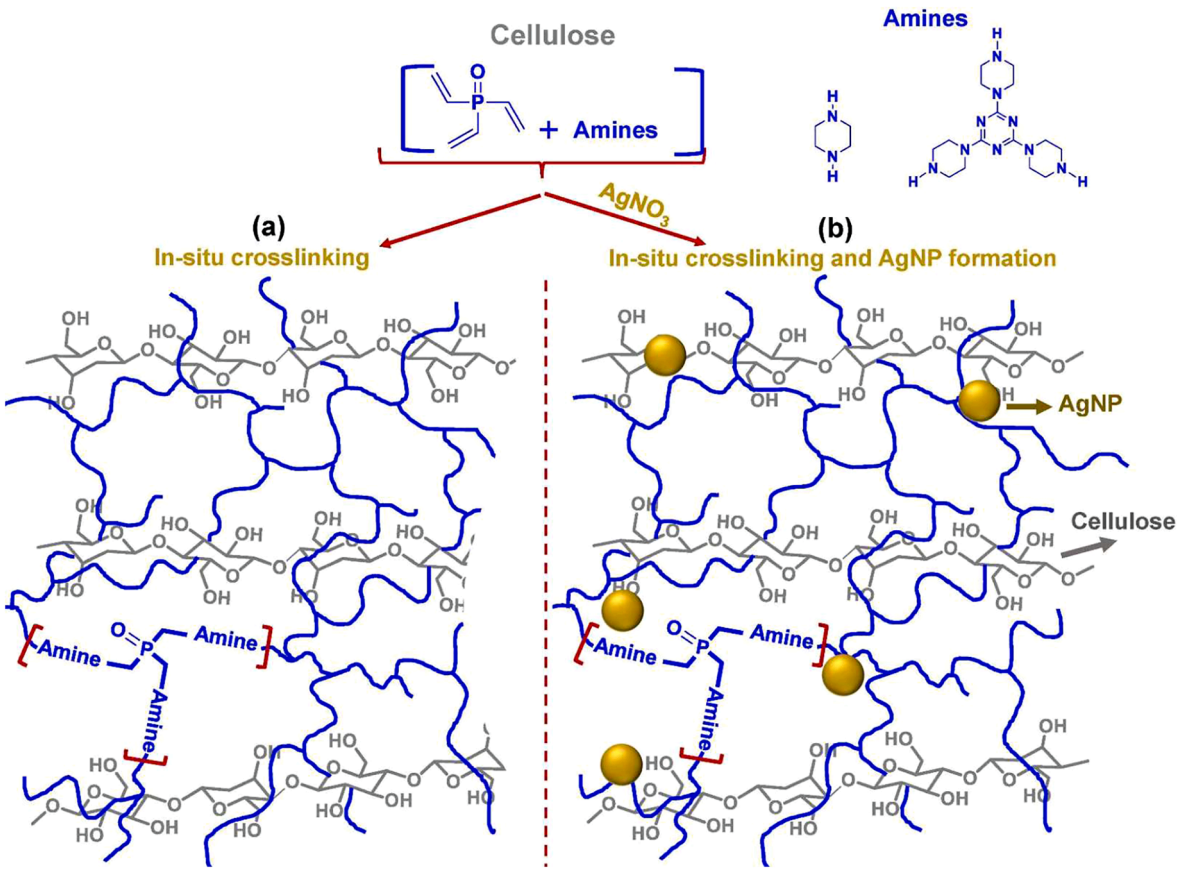

Scheme 1. (a) Phosphine oxide macromolecule (POM) formation within cotton via Michael addition reaction. (b) Simultaneous formation of POM and AgNPs by amine mediated reduction of $AgNO_3$.

protection against fire hazards. Commercially, cellulose textiles are flame retarded by incorporating flame retardant (FR) additives into their bulk during the fiber manufacturing process (suitable for regenerated cellulose fibers) or by special formaldehyde-based finishing treatments (suitable for cotton cellulose) [9–11]. The durability of formaldehyde-based FRs is due to the formation of stable acetal linkage between the FR and the –OH group of cellulose, which can easily withstand more than 50 laundry cycles [12,13]. However, formaldehyde, being a carcinogen, requires manufacturing technologies to be heavily regulated and in some instances, banned [14]. As the majority of cellulose textiles are made from cotton, an environmentally friendly manufacturing process for flame retardation of cotton has been the topic of research over the past few decades [10,15–17]. Thus, there is a need to develop formaldehyde-free processes for flame retardation of cellulose with long term durability.

In recent years, researchers have utilized new FR chemistry based on phosphorus (P), nitrogen (N), and silicon (Si) to impart FR properties to cotton cellulose with varying levels of durability to the laundry process [15–17]. Some of these approaches involve the use of formaldehyde as a building block for the FR synthesis [18–23] or as a crosslinker in the treatment process [24]. FR cellulose with limited durability to laundry can be achieved via the linkage of phosphorus moiety with and without nitrogen to cellulose via a phosphoester bond [19,20,25–27]. In some semi-durable treatments, the phosphorus moiety is linked to cellulose via a "P–O–C bond" [28,29]. Phosphorus moiety, together with methacrylamide has also been grafted to cellulose via radical reactions resulting in treatments stable to 5 laundry cycles [30]. Thus, it is clear that most of these FR treatments on cotton cellulose are either semi-durable or they require the use of formaldehyde at some stage of the manufacturing process for achieving long-term durability. Also, such treatments only address the fire safety of the materials. Whereas, in real-world applications, a multifunctional textile substrate would address multiple threats simultaneously. Especially for firefighters, medical responders, military personnel, and other frontline personnel who are exposed to numerous hazards under different situations, textiles exhibiting both flame retardancy and antimicrobial properties could be very relevant. There are limited studies in the literature which integrates both antimicrobial properties and flame retardancy of cellulose fibers in one treatment. Previously, cellulose was treated with phosphorus and quaternary ammonium-based silicon precursors via a sol–gel technique, but the long-term durability was not examined [31].

Antimicrobial modification of cellulose with silver is well researched and commercial technology for antimicrobial textiles [32–35]. Numerous antimicrobial agents such as metals and their oxides [32–35], antibiotics [36–38], biomolecules [39–43], quaternary ammonium compounds [44,45], halamines [46–48], etc. have been commonly used to render cellulose antimicrobial. Silver nanoparticles (AgNPs) have been proven to be effective against bacteria due to the release of silver ions and the accumulation of AgNPs inside the cell wall, which leads to cell death [49].

FR treatments for cellulose fibers require a weight add on of active ingredient over 30% and significantly influence the textile's comfort properties. The comfort of fabrics can be evaluated by moisture management tests to determine the ease of transport of liquid and water vapor away from the body to the atmosphere. The rapid movement of fluid in the textiles inhibits perspiration soaked next to the skin over a long period and preventing the growth of skin-irritating microorganisms. Moreover, fabrics that transport away moisture from the skin while performing vital functions keep the human body capable of cooling itself and contributing to the overall comfort of the textiles [50].

Thus, a multifunctional cellulose fiber via an in-situ methodology to obtain durable flame retardancy and antimicrobial activity in one-step

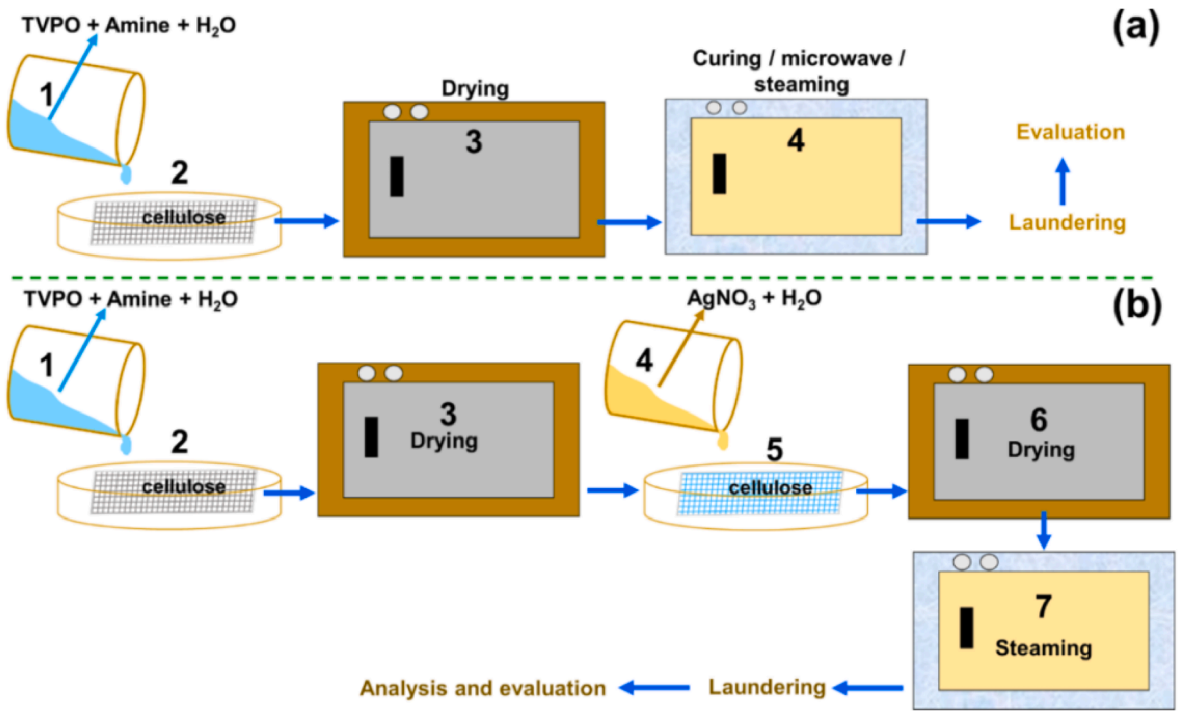

Fig. 1. (a) Procedure outline for FR cellulose via in-situ Michael addition crosslinking (b) Modification of previous procedure to impart flame retardancy and antimicrobial property to cotton by simultaneous Michael addition crosslinking and amine mediated reduction of $AgNO_3$ to form AgNPs.

(Scheme 1) was developed in this work. Cotton cellulose was modified by an in-situ Michael addition crosslinking of trivinyl phosphine oxide and different amines to achieve flame retardancy via a straightforward methodology that can be easily adapted for industrial manufacturing. A similar principle of in-situ synthesis of phosphine oxide macromolecules in various substrates has been recently published in the literature [51,52]. The formation of phosphine oxide macromolecules inside cellulose fibers was confirmed via solid-state NMR analysis. The treated fabrics were evaluated for flame retardancy using the Swiss vertical burning test (BKZ-BV) and limiting oxygen index (LOI). The thermal behavior of the treated cellulose was evaluated using thermogravimetric analysis (TGA) and microscale combustion calorimeter (MCC). The long term durability of the treatments was also assessed (i.e. 50 laundry cycles). The evolved gas analysis was performed using the thermogravimetric analysis, coupled with Fourier-transform infrared spectroscopy (TGA-FTIR) and Direct Insertion Probe-Mass Spectrometry (DIP-MS) to identify the new FR's mode of action. Antimicrobial functionality was also incorporated into the fabric via in-situ AgNP formation to demonstrate the versatility of such a method. The surface topography of the treated fabric was evaluated by Scanning Electron Microscopy (SEM) and transmission electron microscopic (TEM) analysis, which confirmed the formation of AgNPs. A combination of FR and antimicrobial

Table 1
Details of cellulose samples, curing conditions, and % P content.

Crosslinking method (Michael Adducts)	Sample name	Temp. (°C)/Pressure (bar)	Time (h)	P (%) before washing	*P (%) after washing	P-retention (%)
Dry Crosslinking (TVPO + Pip)	D1	120	1	1.46 ± 0.11	0.88 ± 0.18	60
	D2	140	1	1.26 ± 0.08	0.91 ± 0.29	73
	D3	160	1	1.62 ± 0.34	1.29 ± 0.31	80
Microwave Crosslinking (TVPO + Pip)	M1	120	1	2.14 ± 0.29	2.08 ± 0.08	97
	M2	140	1	2.14 ± 0.22	2.01 ± 0.18	94
	M3	160	1	2.08 ± 0.19	1.97 ± 0.00	95
Steaming (TVPO + Pip)	S1	110 (0.4)	0.5	2.06 ± 0.04	1.98 ± 0.03	96
	S2		1	2.05 ± 0.02	2.03 ± 0.01	99
	S3		2	2.12 ± 0.01	2.11 ± 0.00	100
	S4		4	1.91 ± 0.01	1.88 ± 0.03	98
	S5	117 (0.8)	0.5	2.07 ± 0.03	2.01 ± 0.02	97
	S6		1	2.12 ± 0.04	2.06 ± 0.03	97
	S7		2	2.30 ± 0.04	2.27 ± 0.02	99
	S8		4	2.50 ± 0.01	2.50 ± 0.04	100
	S9	110 (0.4)	1	1.11 ± 0.04	1.11 ± 0.06	100
	S10		1	1.56 ± 0.03	1.56 ± 0.04	100
	S11		1	2.23 ± 0.05	2.22 ± 0.09	100
	S12		1	2.67 ± 0.08	2.66 ± 0.14	100
	S13Δ		1	2.16 ± 0.02	2.06 ± 0.02	95
Steaming (TVPO + TPT)	S14	110 (0.4)	1	1.02 ± 0.02	1.00 ± 0.02	98
	S15	110 (0.4)	1	2.04 ± 0.02	1.98 ± 0.03	97
	S16 Δ	110 (0.4)	1	2.06 ± 0.03	2.0 ± 0.03	95

P: phosphorus, **P (%) after washing (5 laundry cycles), Δ P (%) after washing (50 laundry cycles),* Trivinyl phosphine oxide (TVPO), Piperazine (Pip) and 2,4,6-tri(piperazine-1-yl)-1,3,5-triazine (TPT).

properties using in-situ AgNPs for cellulose has not been reported in the literature. The comfort properties of the treated cellulose fabrics were also evaluated.

2. Experimental section

2.1. Materials

Phosphoryl trichloride (99%), vinyl magnesium bromide (1 M in THF), dry THF, piperazine (99%), and silver nitrate ($AgNO_3$, 99%) were obtained from Aldrich and used as received. Trivinyl phosphine oxide (TVPO) and 2,4,6-tri(piperazine-1-yl)-1,3,5-triazine (TPT) were synthesized as per previously reported literature [51]. The plain woven 100% cotton fabric was purchased from Swissatest Testmaterialien AG, St. Gallen, Switzerland, and conditioned for 24 in 65% relative humidity (RH) and 20 °C before use. The synthesis of phosphine oxide polymers (Poly-A and Poly-B) was described in supplementary information (SI-2).

2.2. Methods

2.2.1. NMR analysis

Solid-state ^{13}C and ^{31}P CP-MAS NMR spectra were measured at ambient conditions on a Bruker Avance III 400 NMR spectrometer (Bruker BioSpin AG, Fällanden, Switzerland) with a 4 mm CP-MAS probe. Detailed procedure can be found in SI-1.

2.2.2. Cellulose treatments

The conditioned fabric of the required dimension was taken in a petri dish (Fig. 1) and a freshly prepared equimolar aqueous solution of TVPO and piperazine (volume of the solution = twice the weight of cellulose) was applied evenly on the fabric (Fig. 1). The fabric was then allowed to stand for 15 min with occasional inversions to ensure the homogeneity of the treatment. The quantity of TVPO in the sample was calculated using Eq.1. Where P = desired phosphorus % on fabric, Z = Wt. of fabric (g), considering the molar ratio of TVPO : amine as 1:1 for triazine derivative and 2:3 for piperazine. All fabrics were then oven dried at 60 °C for 10 min, except for microwave crosslinked fabrics (dried for 7 min) to retain the minimum moisture content of 20 wt%.

$$\text{Wt. of TVPO in gram} = P(Z)/(24.14 - P) \quad (1)$$

2.2.3. Crosslinking experiments

(i) ***For Dry crosslinking,*** the treated cellulose fabrics were cured in a preheated oven at 120 ℃, 140 ℃ and 160 ℃ for 1 h as given in Table 1 (Sample **D1-D3** respectively). (ii) In ***Microwave Crosslinking,*** the treated fabrics were placed in a glass tube and cured at at 120 ℃, 140 ℃ and 160 ℃ (**M1-M3** respectively) for 1 h in a SynthWAVE Microwave reactor from MWS Mikrowellen Systeme GmbH, Switzerland. (iii) During ***Steam Crosslinking***, The monomer containing fabrics were mounted on a frame present inside a pressure vessel (Fig. SI-1) at 110℃ and operating 0.4 bar above atmospheric pressure were treated for a different duration (Sample **S1-S4**, Table 1). For comparison, sample **S5-S8** were prepared at higher temperature and pressure (117 ℃, 0.8 bar). After the optimization of the steaming condition, sample **S9-S12** was prepared with different phosphorous content. Finally, sample **S14** and **S15** were prepared using TPT, to study the effect of amines on fabric properties. After steaming, samples were rinsed with warm water for 10 min, drying, and conditioning for 24 h at 65% relative humidity (at 20 °C) before analysis. The details of all crosslinking methods are provided in the Sec. SI-3.

2.2.3.1. In-situ AgNP preparation. The fabrics were treated with an aqueous TVPO-piperazine solution and dried at 60 °C for 5 min (Fig. 1b). The $AgNO_3$ solution was sprayed over the fabric and kept in the dark for 15 min. The required quantity of $AgNO_3$ in the solution was maintained to achieve 0.1 wt% (**SS1**) and 0.75 wt% (**SS2**) of Ag on the final fabric. It was then dried in an oven at 60 °C for 5 min before steaming. After steaming, the fabrics were washed, conditioned and analyzed (Table SI-4).

2.2.4. Long term durability test (Laundry)

The durability of the treatments was evaluated by the AATCC TM-61–1996 standard, which simulates five home laundering cycles. The details of this experiment can be found in sec. SI-4.

2.2.5. Elemental analysis

Phosphorus content of samples was measured using the inductively coupled plasma optical emission spectrometry method (ICP-OES) using a 5110 ICP-OES apparatus (Agilent AG, Basel, Switzerland). Sample preparation for ICP-OES consisted of mixing 200 mg of a sample with 3 mL HNO_3, followed by digestion using a microwave reactor (Synthwave from MLS GmbH).

Energy dispersive X-Ray spectroscopy (EDX) mapping experiments were conducted on a Hitachi S-4800 Scanning Electron Microscope (SEM) operating at accelerating voltages of 20 kV. The cellulose fabrics and char were coated with Au/Pd (5 nm) before analysis.

2.2.6. Thermal analysis and fire tests

Thermogravimetric analysis (TGA) was carried in a NETZSCH TG209 F1 Iris instrument. ~4 mg of sample was heated from 25 to 800 °C at a rate of 10 °C/min. The measurements were performed in N_2 and air with a total gas flow of 50 mL/min.

Limiting Oxygen Index (LOI) values of fabrics were measured on the FTT oxygen index apparatus according to ASTM D2863-97 standard using 140 × 50 mm sample size.

Vertical burning tests of cellulose fabrics were performed according to the Swiss Standard (BKZ-VB). The fabrics in a vertical orientation were exposed to a flame at an angle of 45° for 15 s to record the burn length and time. Five specimens were tested for LOI and vertical burning tests to get an average value. The videos of vertical burning tests of fabrics (blank cellulose, **S9**, **S10**, **S11**, **S12**, **S14**, **S15**, and **SS1**) are available as Supplementary Information (SI).

2.2.7. Microscale combustion calorimeter (MCC)

Heat release rates (HRR) of cotton cellulose were determined using a microscale combustion calorimeter (Fire Testing Technology Instrument, London, UK) following ASTM D7309. ~7 mg of sample was exposed to a heating rate of 1.0 °C/s from 150 to 750 °C in the pyrolysis zone.

2.2.8. Evolved gas analysis

The TGA instrument, coupled with the Fourier-transform infrared spectrophotometer (Bruker Tensor 27), was used to analyze the gasses evolved during pyrolysis. 10 mg of cotton cellulose was heated from 25 to 800 °C at a rate of 10 °C/min^{-1}, and the FTIR spectra of the gases evolved during pyrolysis was recorded with a resolution of 4 cm^{-1} ranging from 4000 to 550 cm^{-1}.

Direct insertion probe mass spectrometry (DIP-MS) analysis was performed for a 1–2 μg sample using the ThermoQuest FINNIGAN apparatus (Austin, TX, USA). The sample was heated from 30 °C to 450 °C at a rate of 50 K/min and 10^{-6} mbar pressure.

2.2.9. Transmission electron microscopic (TEM)

Cotton fibers (~5 mm) removed from **SS1** and **SS2** were placed into molds and embedded in Spurr low viscosity resin. Molds were placed in an oven at 70 °C for 48 h before sectioning in an ultramicrotome (Ultracut F4 Reichert-Jung). First, the block with embedded fibers was trimmed down to an area of interest, followed by cutting ultrathin sections of ~70 nm. Then, ultrathin sections were placed on a Formvar carbon-coated copper TEM grids to record TEM images in a JEOL JEM 2200 fs microscope operating at 200 kV.

2.2.10. Antibacterial assays

The antibacterial property was determined using the model pathogens: *Staphylococcus aureus* ATCC 6538 and *Pseudomonas aeruginosa* DSMZ 1117. The fabrics were sterilized for 20 min under UV (254 nm, 100 μW/cm^2, Kojair Tech Oy, Finland). For the agar diffusion test, 200 μL of exponentially growing bacteria (concentration of 10^5 CFU/mL) was added to Müller-Hinton-Agar (Sigma Aldrich). Sterilized fabrics (5 × 10 mm) were placed on the agar and plates were incubated for 18 h at 37 °C, followed by measurement of the inhibition zone.

For the contact killing test, an exponential growing bacterial culture was prepared in Brain-Heart-Infusion (BHI, Oxoid CM1135) at 37 °C and 160 rpm. The culture was then diluted with phosphate-buffered saline (PBS buffer, Sigma-Aldrich) to 10^6 CFU/mL. 100 μL of bacterial suspension was loaded onto the samples (10 × 10 mm) and incubated at 37 °C for 2 h. The suspension was removed and the samples were washed twice with 450 μL PBS. The removed bacterial suspension and washing solution were mixed, and serial dilutions of the mixture were plated on Plate count agar (Casein-peptone Dextrose Yeast Agar, Sigma Aldrich, 70152). The plates were incubated overnight at 37 °C, followed by colony counting to obtain colony forming units (CFU). Statistical analyses were performed using unpaired and two-tailed Student's *t*-test.

2.2.11. Fabric properties

2.2.11.1. Water Contact Angle (WCA). WCA was measured with water (CHRO-MASOLV, for HPLC, Sigma-Aldrich) at 5 different locations on the fabric surfaces in the ambient condition through a drop shape analyzer (DSA25, Krüss).

2.2.11.2. Fabric appearance. The change in the sample color after treatment was assessed by measuring reflectance of the treated samples using a Datacolor 550 dual-beam spectrophotometer in a wavelength range between 360 nm and 700 nm.

2.2.11.3. Fabric comfort. To evaluate fabric comfort, moisture management properties such as water spreading speed and wettability of fabrics was determined using the Moisture Management Tester (M290 MMT, SDLATLAS). Three fabric samples of 80 × 80mm were prepared and conditioned for at least 24 h in 20 °C and 65% RH before analysis.

2.2.11.4. Strength and bending length. Strength of warp and weft yarns (Fig. SI-20**)** from untreated and treated fabric were determined using a Zwick/Roell Z100 tensile tester with a test length of 5 cm (length of the sample tested). Details of the strength can be found in Sec. SI-12. **Bending length** of the fabric samples were determined as per ASTM 3188 standard. 15 × 2.5 cm fabric strips were prepared in both warp and weft direction to determine the bending length (Sec. SI-12 for details).

3. Results and discussion

3.1. Cellulose treatments and the principle of phosphine oxide macromolecule formation

The hydroxyl groups present in cellulose provide synthetic access points for various FRs that primarily function in the condensed phase. Dehydration reactions catalyzed by acidic species formed from the decomposition of the FR additives are key to flame retardation of cellulose [10]. For most applications in textiles, the durability of such FR treatment to laundry cycles is essential. Despite tremendous progress over the past decades, a commercially feasible, durable, formaldehyde-free FR treatment still eludes the researchers. New FR S12 requires hydrolysis stability and non-leaching behavior to ensure durability throughout laundry treatments. Designing FR moieties to incorporate non-hydrolyzable bonds and network them via a physical or chemical means into the cellulose structure would prevent their leaching.

To fulfill these criteria, a simple strategy of in-situ Michael addition reaction involving phosphorus-based Michael acceptor and nitrogen-based Michael donors was used to synthesize a polymer network within the cellulose (Scheme 1). The cellulose fabrics were treated with a combination of trivinyl phosphine oxide (Michael acceptor), a cyclic amine (Pip or TPT as Michael donors) followed by curing, microwave heating, and steaming to ensure the in-situ formation of phosphine oxide polymeric networks that gets physically trapped within cellulose. A similar principle has previously been demonstrated in the synthesis of phosphine oxide-based pH-sensitive gels [51] and in-situ flame retardant macromolecules in polyamide 6 [52].

Michael addition of TVPO and the amines can be performed at room temperature in aqueous or solvent conditions; however, long curing conditions greater than a few hours [51] are not practical for industrial implementation. Thus, three different crosslinking experiments were performed (i.e., dry heat, microwave irradiation, and steaming) to facilitate faster crosslinking of the Michael adducts inside the cellulose. The detailed procedure of crosslinking experiments is described in Sec. SI-3. Table 1 summarizes details of all cellulose samples prepared using different crosslinking methods. The effect of various conditions, such as crosslinking temperature, time, and pressure was examined. The curing efficacy was estimated by measuring the phosphorus retention (P-retention) of the treated cellulose after standard laundry procedure (5 and 50 cycles). Increasing the curing temperature during dry crosslinking (**D1** to **D3**) improved the P-retention (Table 1) up to 80% at 160 °C. However, high variation in P-retention is possibly due to non-uniform curing. As most of the humidity was removed before the curing process, it may hinder efficient in-situ crosslinking of the Michael adducts, leading to the removal of non crosslinked or partially crosslinked precursors during laundry. As a green processing strategy, microwave-assisted synthesis offers many benefits for its use in the textile industry, such as enhanced reaction rates, higher yields, greater selectivity, and economic. The closed system provided by microwave reactors allowed additional crosslinking experiments to be conducted in humid conditions. Cellulose samples were prepared with a minimum residual humidity (20 wt%) and modified by microwave-crosslinking.

As seen from Table 1 (**M1** to **M3**), a higher P-retention (>90%) could be obtained for all treated cellulose samples, albeit with higher variation similar to the samples prepared by dry crosslinking. Improved P-retention, even at a lower crosslinking temperature (120 °C), is attributed to the residual humidity and microwave irradiation, which facilitate efficient Michael addition of adducts. The partially dried fabric was placed in the glass tube in a vertical orientation for microwave crosslinking. This led to the migration of Michael addition precursors to the bottom of the sample and a P-content variation from the top (lower) to the bottom (higher).

The steam crosslinking was performed in a simple setup (Fig. SI-1) and a high P-retention (>95%) with low-variation was observed for all samples (**S1**-**S16**). This demonstrates the uniformity of the steam crosslinking method. In the steam crosslinking procedure, the P-retention was independent of the curing temperature (pressure) and curing time (**S1-S4** vs. **S5-S8,** Table 1). A crosslinking temperature of 110 °C and a curing time of 30 min was optimum to obtain high P-retention, providing reasonable conditions to adopt in an industrial textile process. Only in the case of TPT, ethanol was used as a solvent due to its poor solubility in water and high P-retention was observed, similar to other steam crosslinked samples. The P-retention for cellulose fabrics reported in Table 1 is after 5 laundry cycles. To further examine the durability of the treatments, 50 laundry cycles were performed (**S13**). Interestingly, 95% P-retention after 50 laundry cycles demonstrated the long term stability of the FR chemistry employed in this work, which is comparable to the commercially available formaldehyde-based FR for cotton fabrics.

To verify the formation of in-situ phosphine oxide macromolecules within the cellulose matrix, a solid-state NMR study was performed on the treated cellulose. For comparison, the crosslinked polymer (Poly-A) was synthesized after solid-state polymerization of TVPO and piperazine

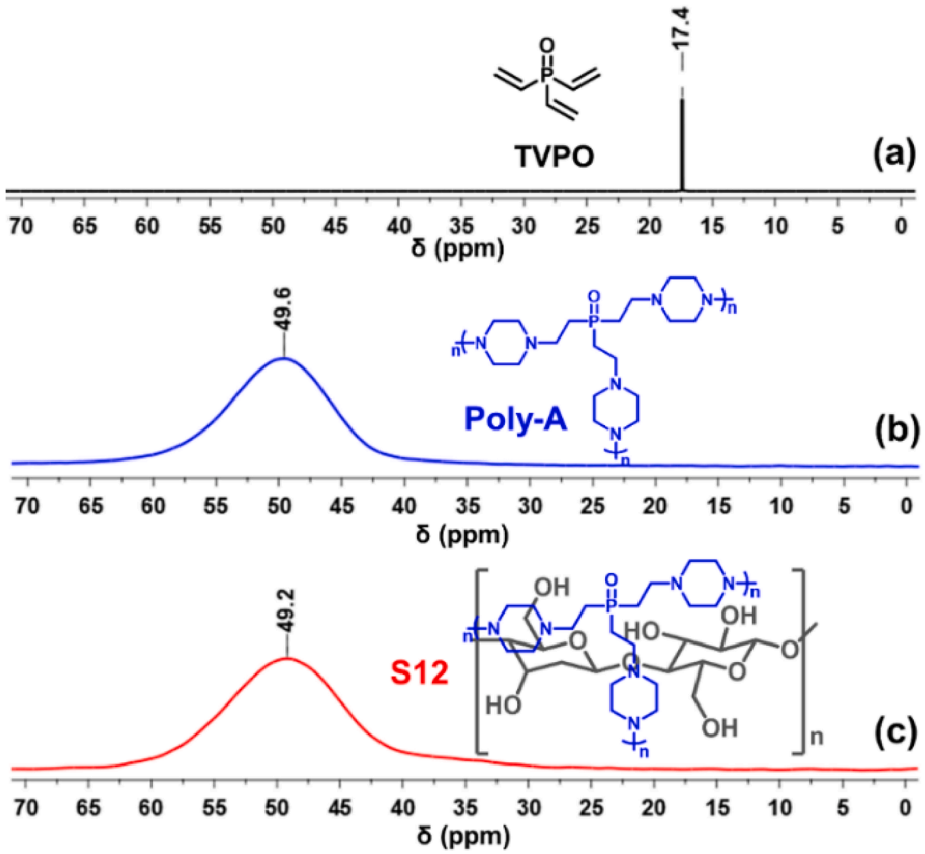

Fig. 2. (a) ^{31}P NMR spectra of TVPO in $CDCl_3$ (b) ^{31}P MAS NMR spectra of Poly-A and (c) **S12**.

Table 2
Summary of small-scale fire tests.

Samples	P (%)	BKZ-VB[a] Test			LOI %± 0.2
		After Flame (sec)	Burning Length (cm)	Pass/ Fail	
Blank	—	14.3 ± 0.5	burns	Fail	18.7
S9	1.11 ± 0.06	25.3 ± 0.9	burns	Fail	23.1
S10	1.56 ± 0.04	20.0 ± 2.5	burns	Fail	24.5
S11	2.22 ± 0.09	0	7.6 ± 0.7	Pass	27.0
S12	2.66 ± 0.14	0	6.2 ± 1.3	Pass	28.4
S14	1.00 ± 0.02	17.0 ± 1.4	burns	Fail	25.15
S15	1.98 ± 0.03	0	3.4 ± 0	Pass	27.41
SS1	2.08 ± 0.08	0	7.7 ± 0.2	Pass	26.9

[a] Swiss standard vertical fire test. All Samples for the fire tests were exposed to 5 wash cycles, dried and conditioned before the fire tests. Details of **SSI** can be found in Table SI-4.

in the absence of cellulose (See SI-2 and S1-5). Fig. 2 shows the ^{31}P NMR data of TVPO, **S12,** and crosslinked polymer Poly-A. The broad phosphorus resonances centered at δ 49.6 ppm and 49.2 ppm (Fig. 2b) in the ^{31}P MAS NMR spectra of Poly-A and **S12,** respectively, can be assigned to polymer-bonded phosphorus atoms. The disappearance of the TVPO phosphorus peak at δ 17.4 ppm in ^{31}P NMR spectra (in $CDCl_3$, Fig. 2a) confirms the complete conversion of the starting material [51,52]. The ^{13}C and ^{31}P CP-MAS NMR spectra of blank cellulose, poly-A, Poly-B, **S12** and **S14** are presented in SI5 (Fig. SI-2 to SI-7).

3.2. Small scale fire tests

Untreated cellulose-based materials are readily combustible and require the application of flame retardants as a safety measure. These fireproof treatments are often based on various phosphorus chemistries, which have enhanced fire performance [10]. When exposed to fire, phosphorus-based flame retardants in cellulose will decompose to form an acidic phosphorus species that catalyzes char formation [53,54]. The char formed acts as a thermal barrier against heat and thus protects the underlying polymer. This mode of action exhibited by phosphorus-based flame retardants is referred to as the condensed phase activity.

Vertical flammability test (BKZ- VB) and LOI were performed on the treated cellulose fabrics to mimic small scale fires (Table 2). An increased concentration of phosphorus in the treated cellulose led to an improved fire performance (**S9-S12**), which is reflected as increased LOI values and reduced char length in the BKZ-BV test. For a P-content >2 wt % a pass in the BKZ-VB test and an LOI value >27% was achieved. Post-fire test (BKZ-BV) examination of the remaining residues revealed increased char formation for all treated fabrics (Fig. SI-9). The untreated fabric burned completely (Video1-Cellulose blank), leaving no char residue. Even though **S9** and **S10** are not self-extinguishing (Video2-S9 and Video3-S10), a significant char remained after the fire test. Concentrations of phosphorus >2 wt% improved the quantity of the char and self-extinguishment of the fabrics (Video4-S11, Video5-S12, and Video7-S15). Likewise, cellulose-containing TPT (**S14** and **S15**) exhibited similar results in the small scale fire tests (Table 2).

3.3. Microcombustion calorimetry (MCC)

Micro combustion calorimetry (MCC) was used to estimate functionalized cellulose's fire performance (Fig. 3, Table 3). As shown in Fig. 3 and SI-10, all treated samples displayed a lower peak heat release

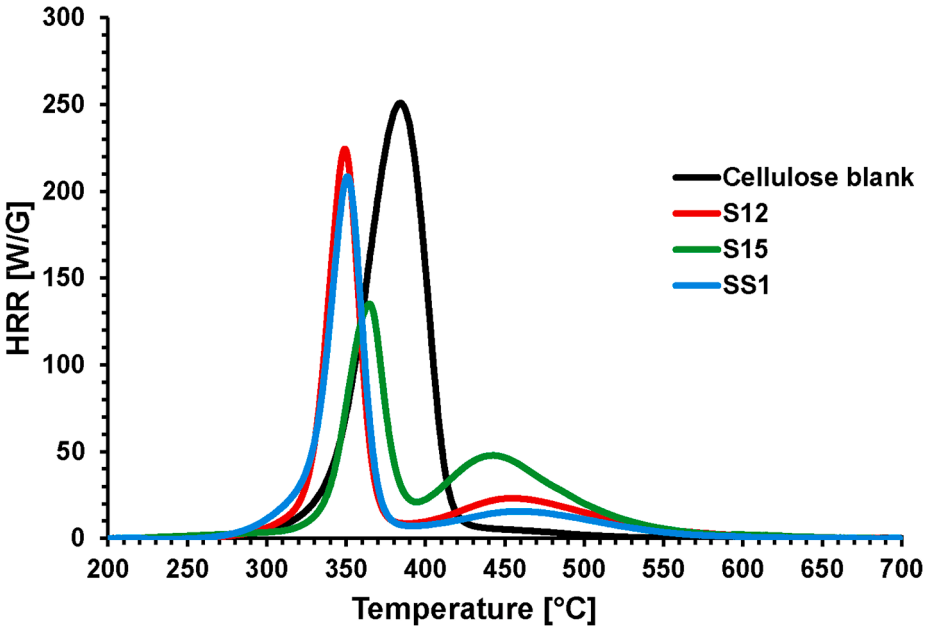

Fig. 3. Heat release rate (HRR) of **Cellulose blank**, **S12**, **S15** and **SS1** were measured using MCC.

Table 3
Heat release profile of treated cotton cellulose.

Sample	P (%)	T_{max} (°C)	pHRR ($W.g^{-1}$)	THR ($kJ.g^{-1}$)	HRC (J/g-K)	Residue (%)
Blank	—	388.3 ± 1.5	252.1 ± 1.4	12.6 ± 0.0	249.6 ± 0.9	8.4 ± 0.7
S9	1.11 ± 0.06	353.2 ± 4.2	218.3 ± 5.8	9.0 ± 0.1	220.0 ± 9.5	22.6 ± 0.9
S10	1.56 ± 0.04	352.0 ± 0.4	237.6 ± 2.8	8.3 ± 0.5	238.0 ± 4.5	26.8 ± 0.3
S11	2.22 ± 0.09	345.0 ± 2.2	226.7 ± 5.3	8.3 ± 0.1	223.3 ± 4.7	27.8 ± 0.4
S12	2.66 ± 0.14	348.2 ± 1.2	231.0 ± 12.9	8.5 ± 0.1	228.6 ± 12.2	29.6 ± 0.4
S14	1.00 ± 0.02	365.2 ± 1.9	186.1 ± 8.5	9.4 ± 0.2	184.0 ± 8.5	30.7 ± 0.8
S15	1.98 ± 0.03	356.9 ± 4.0	169.4 ± 12.5	8.9 ± 0.0	144.0 ± 42.5	32.5 ± 8.4
SS1	2.08 ± 0.08	350.5 ± 2.8	211.5 ± 6.1	7.9 ± 0.1	207.3 ± 7.1	40.1 ± 0.7

pHRR = peak of Heat Release Rate, THR = Total Heat Release, HRC = Heat Release Capacity.

rate (pHRR), heat release capacity (HRC), total heat release (THR), and higher residue compared to the untreated cotton (Table 3). Lower temperature for pHRR (T_{max}) in treated samples is due to the catalyzed decomposition of cellulose by acidic phosphorus species formed during the thermal decomposition of phosphorus compounds [55–57]. Increased P-content in cellulose leads to higher catalytic activity and results in lower HRC and T_{Max}, similar to the observation made in previous research [55]. Compared to piperazine containing cellulose (**S10** and **S11**), TPT treated samples (**S14** and **S15**) at a similar P-content exhibited lower pHRR, possibly due to synergistic interaction between the triazine moiety in TPT with the phosphorus moieties [57].

3.4. Thermal data and evolved gas analysis

TGA studies of treated cellulose were undertaken to understand the decomposition behavior and gain insights into possible mode of action of the in-situ formed phosphine oxide macromolecules. The relevant TGA data of treated cellulose in inert and oxidative conditions are summarized in Table SI-5 and the curves are presented in Fig. 4, Fig. SI-11 and 12. All treated cellulose have lower T_{donset}, and T_{dmax} (Table SI-5) but significantly higher residue at 800 °C compared to blank cellulose. Poly-A and Poly-B exhibited a very high thermal stability (~360 °C and ~400 °C respectively) and a high char residue of ~30% (Poly-B). High thermal stability is typical behavior of crosslinked polymer systems [58,59] and higher residue could be due to the formation of thermally stable O-P-N-based inorganic polymer in N_2 and air, which is a typical effect of phosphorus based FR on cellulose [10,55,57]. Poly-B owing to the thermally stable triazine moiety, exhibits higher thermal stability compared to Poly-A.

The decrease in decomposition temperatures with improved char formation in treated cellulose was more pronounced in samples with higher P-content (**S9-S12**), highlighting the acid-catalyzed decomposition of cellulose. The phosphorus compounds decompose to produce phosphoric acid substructures and catalyzing cellulose decomposition to produce carbonaceous residues. In addition, base-catalyzed decomposition of cellulose is also possible due to amines moieties (i.e., piperazine and triazine moieties) in the phosphine oxide macromolecules [60]. For the treated cellulose, lower residues at 800 °C was observed in the air compared to those in N_2 atmospheres, which may be due to lower oxidative stability of the char [55,56].

3.5. Mechanism studies

It is clear from the MCC and TGA data that treated cellulose exhibits higher char formation compared to the untreated cellulose. Besides, in small scale fire tests (BKZ-BV, Fig. SI-9) considerable char formation was observed for the treated cellulose. The chemical composition of such residue can provide useful information on the fate of important elements like P, O, and C after the combustion process. The elemental composition of char obtained after vertical burning tests (BKZ-BV) of five samples (**S9**, **S12**, **S14**, **S15**, and **SS1**) was determined via EDX analysis (Table SI-6 and Fig. SI-13). For all residues, C, P, and O were the primary elements detected. With increasing initial P-content, decreased carbon, increased phosphorus, and oxygen contents were observed for treated cellulose. The decomposition of the phosphine oxide macromolecules leads to phosphorus species, which could crosslink to assist in forming a continuous char layer. Interestingly, nitrogen could only be detected for triazine containing amine samples (i.e., **S14**, **S15**), clearly indicating the

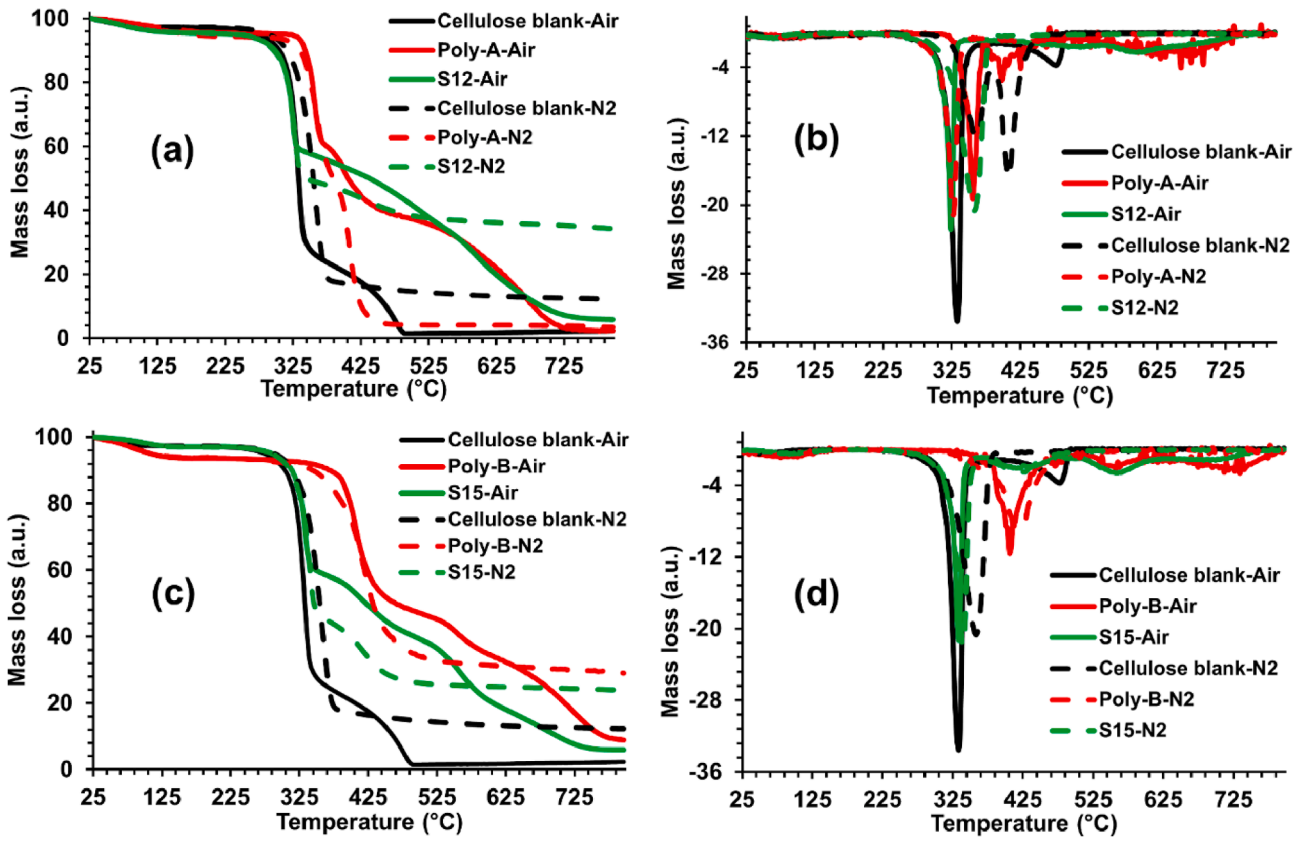

Fig. 4. (a) TGA (b) DTG curves of Cellulose blank, Poly-A, **S12** under Air/N_2 (c) TGA (d) DTG curves of Cellulose blank, Poly-B, **S15** under Air/N_2. T_{donset} (°C): the temperature of 97%, excluding moisture. T_{dmax} (°C): the temperature of the maximum mass loss rate is measured as the DTG peak maximum.

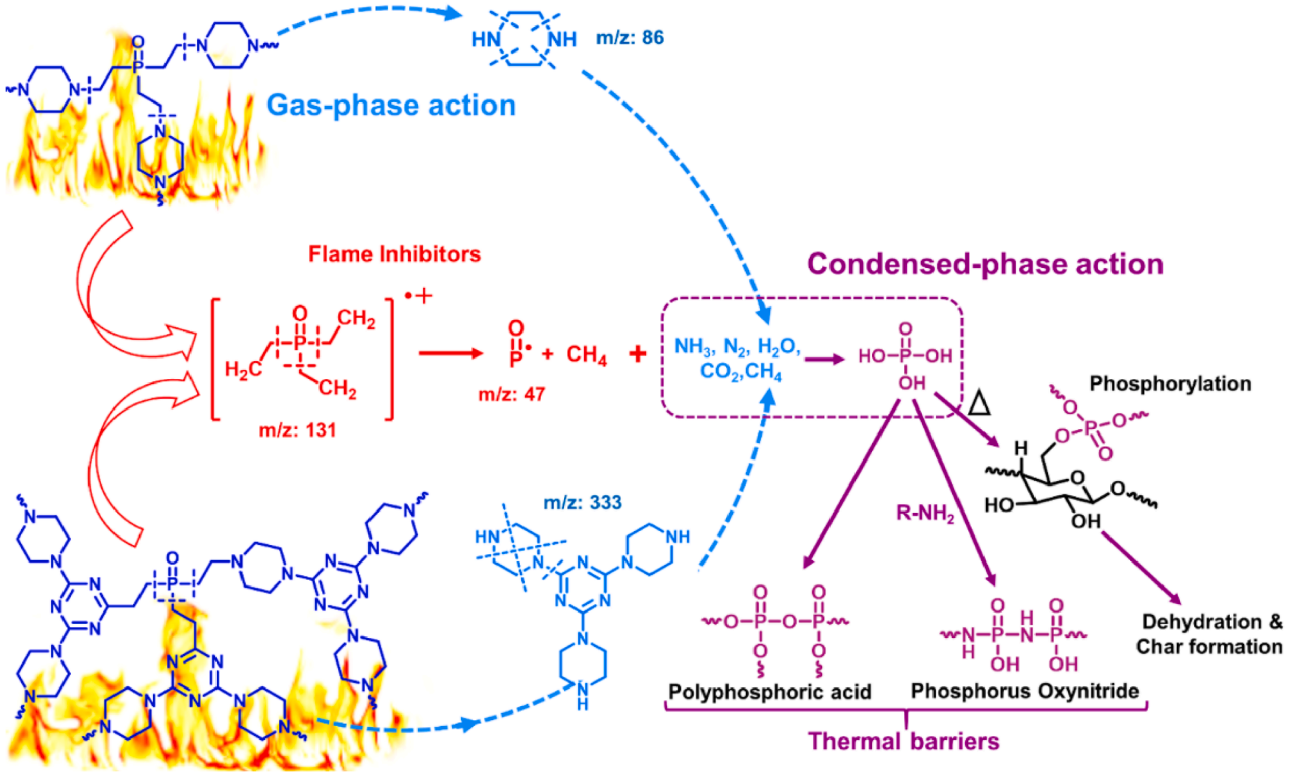

Scheme 2. Proposed pathways for the gas and condensed phase mode of action of treated cellulose.

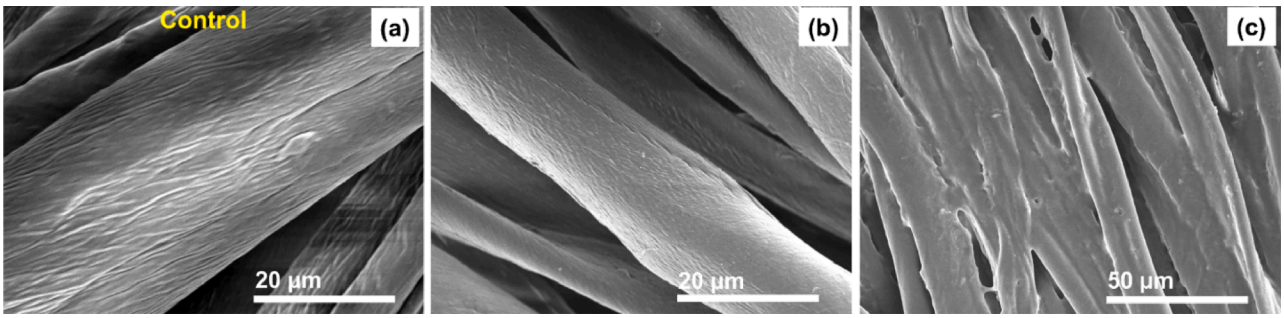

Fig. 5. SEM image of (a) untreated cotton fabric, (b) **S12** and (c) **S15**.

difference in the condensed phase activity of the triazine based phosphine oxide macromolecules compared to the piperazine based phosphine oxide macromolecules. The morphology of char left after the burning was evaluated and for simplicity, only the microscopic image for **S12** is presented in Fig. SI-13. One can see that the charred fibers on the fabric residue are non-voluminous, thus it is unlikely that the FR treatment has intumescent characteristics.

The evolved gas analysis was performed using TGA-FTIR and DIP-MS to understand the FR mode of action in treated cellulose. Briefly, the TGA-FTIR data (Fig. SI-14 and 15) of treated cellulose confirmed an increased formation of nonflammable gasses like H_2O, CO_2, and reduction in flammable gasses like (carbonyl compounds, hydrocarbons, and CO). Such observation is a characteristic of condensed phase action of phosphorus compounds in cellulose [56,57]. The formation of phosphorus-based volatiles was confirmed by phosphoryl peak at 1268 cm^{-1} [61]. Further, DIP-MS of treated cellulose (Fig. SI-16) confirmed the formation of phosphorus (PO*, triethyl phosphine oxide) and nitrogen (piperazine and TPT) species in the gas phase. The formation of volatile phosphorus species indicates their possible gas-phase activities.

Based on these observations, decomposition mechanisms of the treated cellulose is proposed in Scheme 2. Phosphine oxide macromolecules in **S12** and **S14** decompose to yields triethyl phosphine oxide radical, piperazine (**S12**) and TPT (**S14**) in the gas phase. In the next stage, piperazine or TPT decomposes to form ammonia (NH_3) [62], nitrogen (N_2), H_2O, CO_2 and alkane. Furthermore, the triethyl phosphine oxide fragment of **S12** and **S14** decompose to produce alkane and $PO^{\bullet}$. The $PO^{\bullet}$ could remain in the condensed phase to produce phosphoric acids and polyphosphoric acid, thus reinforcing the condensed phase activity. The $PO^{\bullet}$ can also work in the gas phase by recombining H and OH radicals [63,64]. Amines catalyze acidic phosphate intermediates

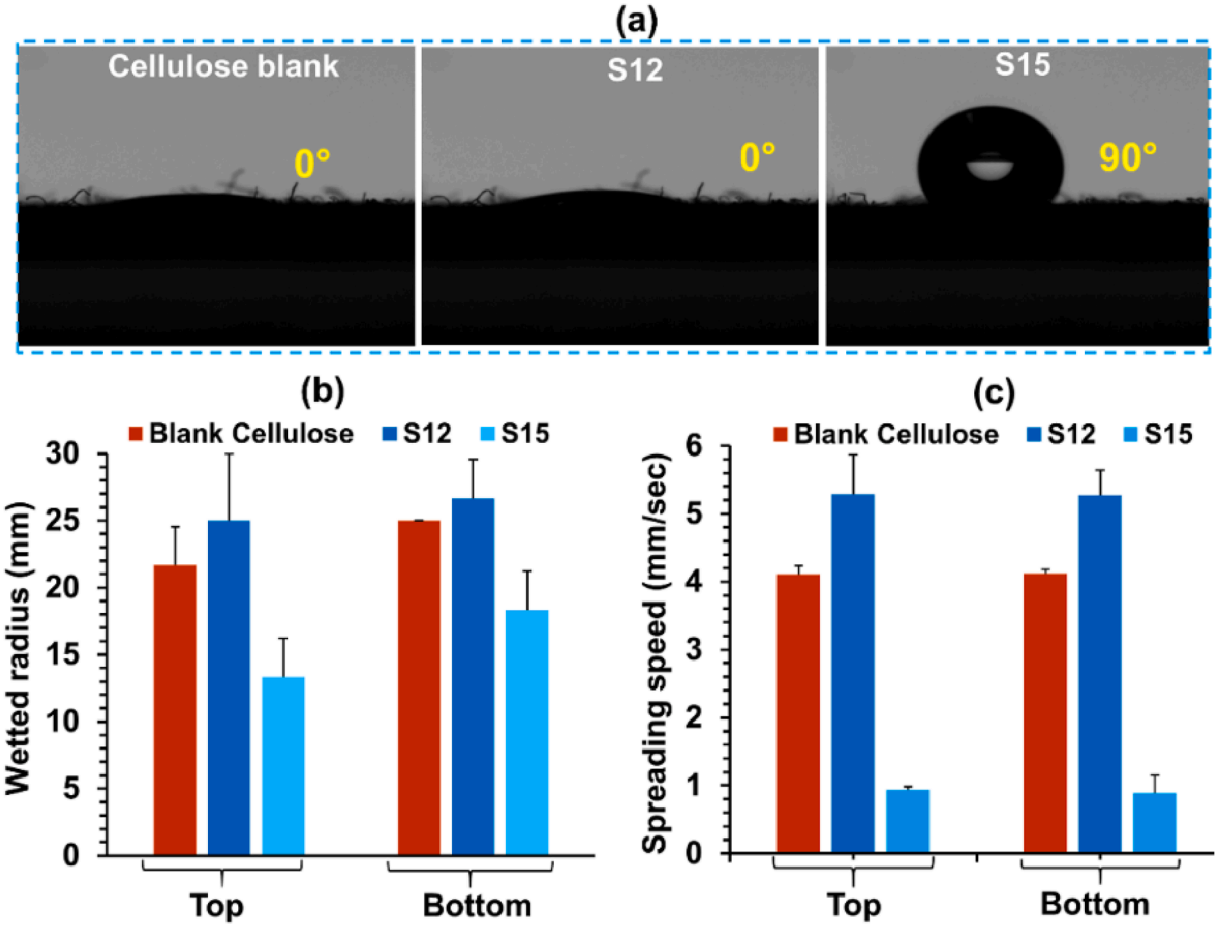

Fig. 6. (a) Water contact angles, (b) Maximum wetted radius and (c) water spreading speed both surface (top and the bottom) of Cellulose blank, **S12** and **S15**.

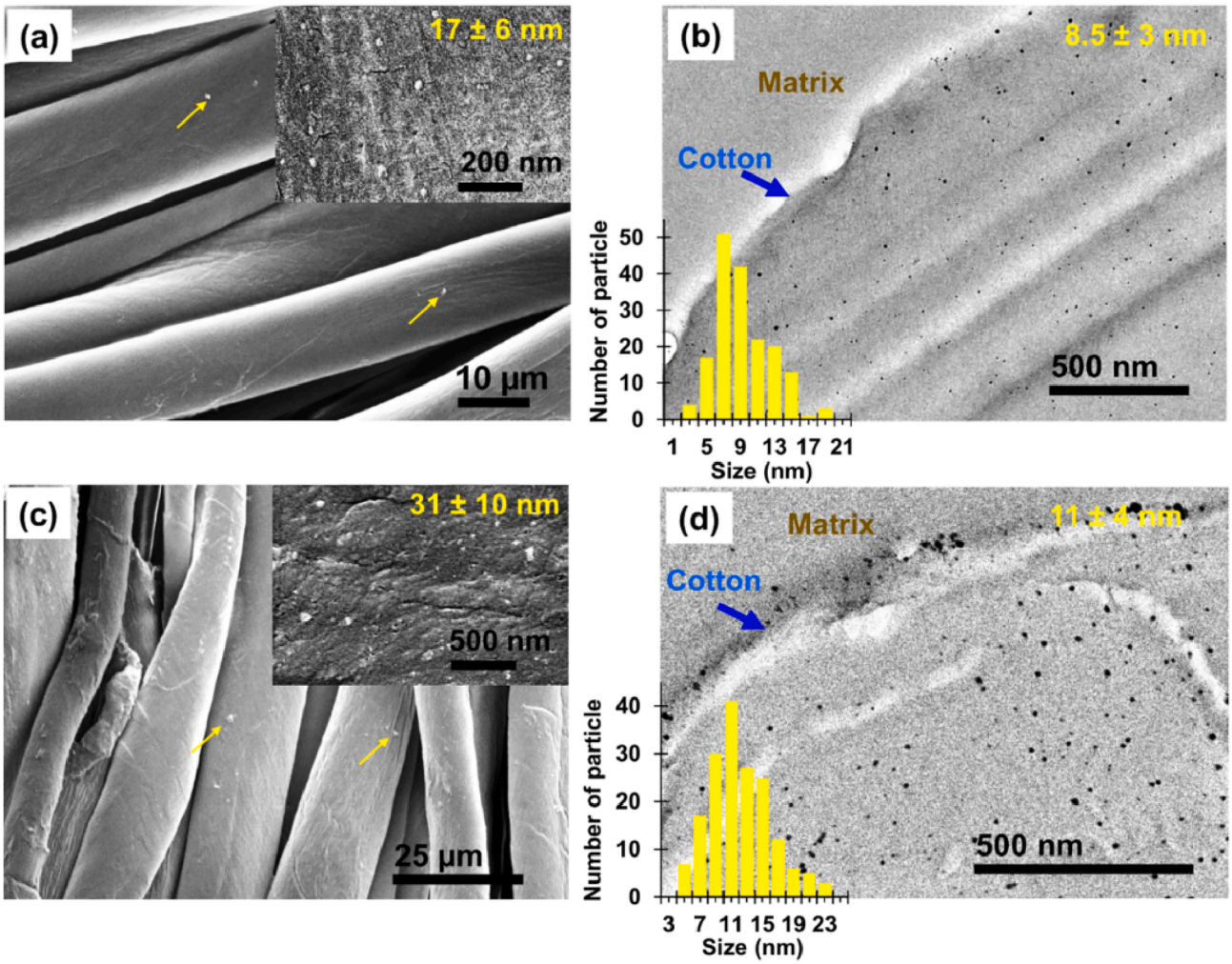

Fig. 7. SEM image of (a) **SS1** and (b) corresponding TEM image. (c) and (d) SEM and TEM image of **SS2**. High magnification SEM images of the sample surface are shown as insets in (a) and (c).

formation leads to cellulose phosphorylation and yields polyphosphoric acid, which assists in the condensed phase activity. Moreover, the amines can also react with polyphosphoric acids to form phosphorus oxynitride, reinforcing it, and acting as an excellent thermal barrier [57].

3.6. Fabric properties after treatment

3.6.1. Fabric morphology

The phosphine oxide macromolecules are expected to form primarily inside the cellulose without influencing any surface characteristics. Thus, the SEM analysis was performed to get further insight into surface morphology of treated samples. No difference in surface morphology of blank cotton cellulose and **S12** was observed in the SEM analysis (Fig. 5a and b), which indicates that phosphine oxide macromolecules are formed inside the cellulose fibers due to the diffusion of precursors into the cellulose matrix before crosslinking. The in-situ formation of crosslinked networks is already highlighted by complete P-retention even after 50 laundering cycles and solid-state NMR analysis. On the contrary, coating observed in the SEM image of **S15** (Fig. 5c) is due to poor diffusion of TPT (insoluble in water) into the matrix, resulting in the formation of crosslinked networks on and within the fibers.

3.6.2. Fabric comfort, appearance and strength

It is important to examine the effect of FR treatments on the comfort properties of the textiles. Use of FR above 20–30 wt% of the material for efficient fire protection results in a possible change in the fabric's moisture absorption and transport capacity, and affecting the comfort properties. Thus, comfort properties were evaluated by measuring the wettability and moisture transport characteristics of fabric samples. The wettability of the cellulose textiles measured as water contact angle (WCA, Fig. 6a) indicated the hydrophilic behavior of the untreated cotton and **S12** (WCA of 0°). Whereas, WCA of 90° in **S15** indicates a hydrophobic nature of the treatments (Fig. 6a).

The moisture management properties were investigated to assess critical aspects of wear comfort of protective clothing [50]. The water spreading speed and maximum wetted radius were taken as measures for moisture transport and absorption, respectively (Fig. 6b and c). The maximum wetted radius reflects the moisture spreading distance for fabric and indicates its moisture uptake properties. Good moisture uptake properties are important for moisture absorption from the environment and control the clothing microclimate. This is critical to prevent the growth of skin-irritating bacteria, yeast, and fungus. A fast-spreading speed contributes to the quick distribution of liquid in the fabric, contributing to a good drying behavior of the fabric. This is important to keep the water vapor gradient within the garment to maintain the body's evaporative cooling and, on the other side, to remove moisture clothing to maintain protective properties. Moisture management parameters were measured at the top and bottom of the blank and treated cellulose textiles and are classified according to the literature [65]. The higher wetted radius for **S12**, compared to the blank fabric and **S15** can be due to the hydrophilic nature of the Poly-A. **S15**

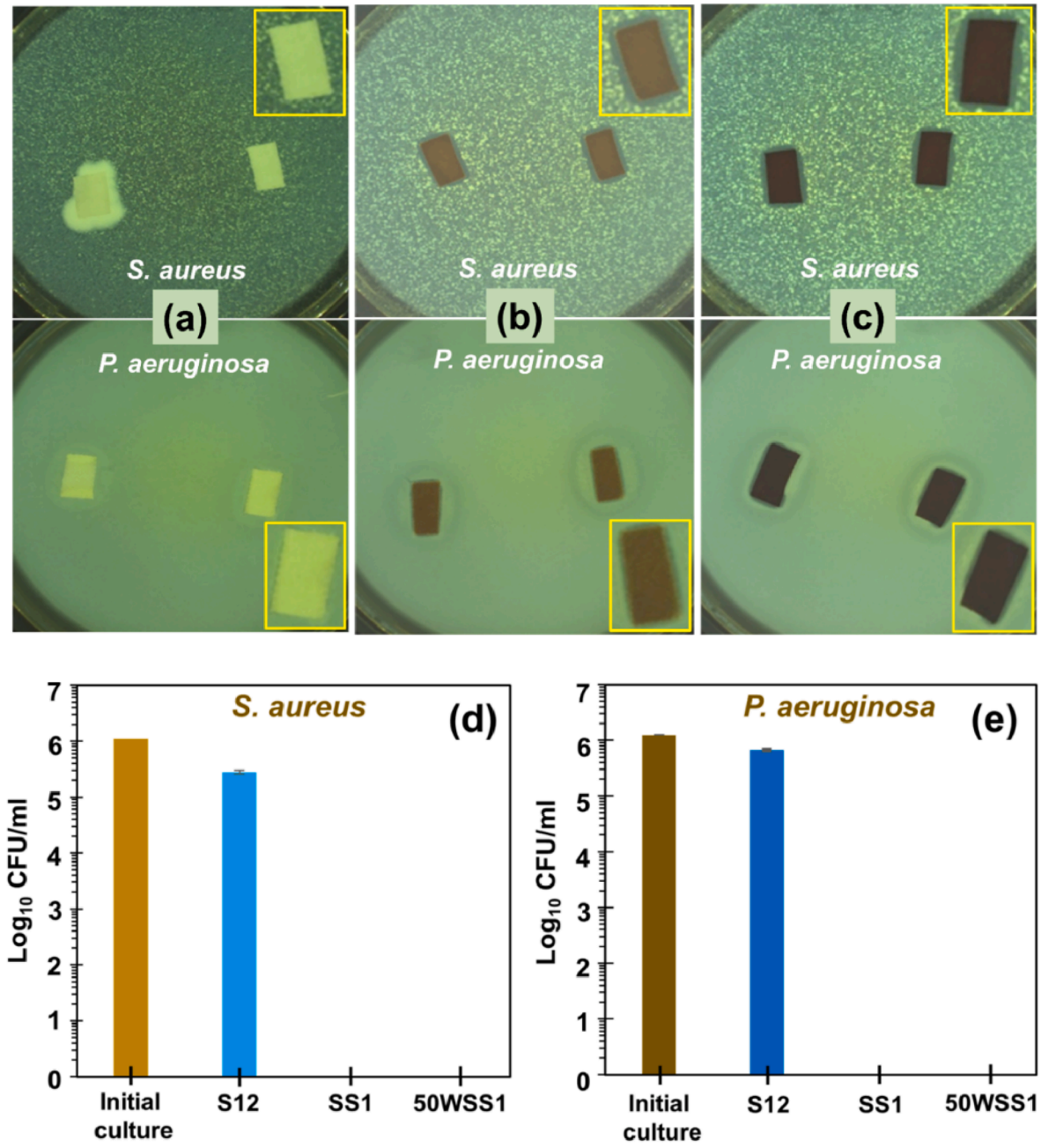

Fig. 8. Antimicrobial activity of (a) **S12**, (b) **SS1** and (c) **SS2** determined by agar diffusion test using *S. aureus* and *P. aeruginosa*. Contact killing of (d) *S. aureus* and (e) *P. aeruginosa* by **S12**, **SS1** and **50WSS1** (**SS1** after 50 launderings). Standard deviations derived from three replicates are shown as Error bars.

showed a medium wetted radius, which might be due to the hydrophobic nature of Poly-B. Furthermore, the liquid spreading speed contributed to quick evaporation and was classified as very fast for **S12** (5.3 mm/sec) and pristine cellulose (4.1 mm/sec). The spreading rate on **S15** is classified as very slow.

Cellulose fabrics tend to turn yellow when subjected to heat [66] and alkaline conditions [67], adversely impacting their visual aesthetics. To ascertain the effect of the novel FR treatment on the fabric's appearance, the reflectance was measured using a spectrophotometer (Fig SI-19). Interestingly, the reflectance value of **S12** was equal to that of untreated fabric within the wavelength range of 500–800 nm, confirming no discoloration during the treatment. On the other hand, the lower reflectance of **S15** at all wavelengths (Fig. SI-19b) indicates a slight yellowing of the fabric. This could be due to small impurities (ppm levels) present in TPT after its synthesis.

From SEM and comfort analysis, it is clear that FR treatment using piperazine (**S12**) maintains the cotton fabric's desired properties. To further evaluate the potential impact of the FR treatment, mechanical properties of warp and weft yarns of the treated fabrics (**S12**) were evaluated and presented in Sec. SI-12. As shown in Table SI-7, no adverse effect of FR treatment on the mechanical properties was observed. The bending length of a fabric that indicates its stiffness was thus measured and sample **S12** has a slightly higher value than the untreated fabric (Table SI-7), indicating a marginal increase in the fabric's stiffness after FR treatment.

3.7. *In-situ silver nanoparticle formation and antibacterial property*

By exploiting reducing ability of amines to form AgNPs from silver salts [68,69], a multifunctional approach to integrated flame retardant

Table 4
Comparison between the state of art literature data with the treatment carried out in this work.

Flame retardants	Durability			LOI (%) 0 LCs	Whiteness Index (%)	Comfort property	Multifunctional	Ref.
	WG (%) 0 LCs	WG (%) 50 LCs	Wt. loss (%)					
PipEPO	21.8	20.6	5.8	26.9[a]	94.4	Good	✓	This work
TPTEPO	44.3	42.5	3.9	27.4[a]	92.4	Good	✓	This work
AgNWs	31.7	NG	NG	37.0	NG	NG	✓	[17]
C_3-PDMS-TiO_2	16.2	14.6	9.9	29.0	yellowish	NG	✓	[16]
DCA	NG	NG	NG	NG	NG	NG	NO	[15]
AGATMPA	24.5	14.4	41.2	45.5	NG	NG	NO	[21]
FR-PA	33.3	25.1	24.6	40.5	NG	NG	NO	[22]
ATPMPA	26.1	14.7	43.8	43.6	80.8	NG	NO	[23]
ASXPEA	21.2	11.6	45.3	45.2	81.0	NG	NO	[27]
ATEPAHP	26.0	12.0	53.8	40.5	NG	NG	NO	[20]
ACMPEP	33.4	21.3	36.2	34.4	82.3	NG	NO	[19]
AHEDPA	25.2	13.9	37.5	42.6	NG	NG	NO	[26]
AEGDP	23.7	14.8	37.5	41.0	NG	NG	NO	[25]
DHTP	60.4	54.5*	9.7	27.2	NG	NG	NO	[29]
cyclotriphosphazene	9.4	9.3*	1.53	21.2	NG	NG	NO	[28]

*30 after washing cycles, [a]after 5 washing cycle, Not given (NG).

and antimicrobial properties within cellulose was explored. In contrast to conventional methods, this route eliminated the use of any additional reducing agent for preparation of AgNPs [70,71] and enabled simultaneous in-situ formation of TVPO-piperazine network and AgNPs (Sec. 2.3). Cellulose treated with $AgNO_3$ maintained their white color even after drying (Fig. SI-2), while yellow color after steaming indicated the formation of AgNPs (Fig. SI-2). The actual silver content in **SS1** and **SS2** were 0.08% and 0.75% respectively (Table SI-4). The durability of silver treatment was confirmed by subjecting the **SS1** to 50 laundering cycles (AATCC 61–2013). Interestingly, the sample displayed excellent Ag-retention and P-retention even after 50 home laundering cycles (Table SI-4). The fire performance of the fabric was not affected by the presence of AgNPs (**SS1**). As shown in Video V8 of SI and Table 2, **SS1** exhibited excellent flame retardancy similar to **S11**.

To confirm the presence of AgNPs in the treated cellulose, SEM and TEM analyses were performed. SEM and TEM analysis of **SS1** confirmed the presence of AgNPs on and within the fiber with an average particle size of 17 ± 6 nm 8.5 ± 3 nm, respectively (Fig. 7a and b). From the TEM image (Fig. 7b), it can be seen that number of AgNPs and their size tends to increase towards the surface of the fiber. It can be attributed to the migration of Ag^+ ions towards the surface during drying followed by the formation of AgNPs during steaming. This also explains the presence of larger AgNP on the surface of the fibers than in its interior. Increasing the $AgNO_3$ loading to 0.75% (**SS2**), an increase in particle size to 11 ± 4 nm was observed (Fig. 7d). Similar to **SS1**, more number of AgNPs with a larger size were observed near the surface of the fiber in case of **SS2**.

The antibacterial property of the cotton fabric with an amine-based phosphine oxide polymer and silver nanoparticle was evaluated by agar diffusion test using *S. aureus* and *P. aeruginosa*. Bacterial growth on and around **S12** fabric samples was observed in both cases (Fig. 8a). Unlike published reports [72,73], no zone of inhibition was observed for *P. aeruginosa* exposed to fabric samples with AgNPs (Fig. 8b and c, lower panels) and only slight inhibition of *S. aureus* growth adjacent to the sample edges (Fig. 8b and c, upper panels). The absence of a zone of inhibition can be attributed to a lack of sufficient silver release from the samples. A similar observation, even in a sample with high Ag-content (**SS2**) highlights the stabilizing effect of a crosslinked Poly-A network present in the composite cellulose (Fig. 8c). Very low loss of silver even after 50 laundering cycles also confirmed the stabilizing effect of phosphine oxide macromolecule (Table SI-4).

To elucidate the antibacterial efficacy of fabrics, contact killing of both bacteria was carried out using the sample with 0.1% Ag before (**SS1**) and after 50 laundry cycles (**50WSS1**) [74,75]. The bacterial suspension was directly loaded on the **SS1** and **50WSS1**, followed by incubation at 37 °C for 2 h (Sec. 2.7). Similar to the agar diffusion test, no killing was observed in the case of **S12**. Interestingly, the complete killing of both bacterial strains by **SS1** and **50WSS1** during contact killing tests (Fig. 8d and e) highlights the antibacterial efficiency and its durability. It is worth mentioning that excellent antibacterial property with low Ag-release is highly desirable for protective materials with minimum exposure to nanomaterial pollution.

Finally, flame retardant cellulose prepared in this work is compared with the recently reported state of art FR treated cellulose (Table 4). Properties such as durability of the treatment, fire performance (LOI), whiteness index (%), comfort, and multifunctionality of the treated fabrics are considered for comparison. It can be seen that (Table 4), the novel FR treatment for the cellulose developed in this work can achieve durable fire performance (after 50 laundry cycles) and excellent comfort property without discoloration of the fabric. Additionally, the novel method offers a possibility to impart excellent antimicrobial property along with fire performance in a single step, which is not common among the recently reported state of art methods.

4. Conclusion

Formaldehyde-free flame retardant treatments for cotton cellulose have been a challenge for researchers over the last few decades with no clear solution which has been commercialized. In this work, a durable flame retardant cellulose was developed via in situ Phospha-Michael addition crosslinking reaction using TVPO and cyclic amines (piperazine or TPT) as precursors. A simple application from an aqueous solution followed by crosslinking under the steam of the treated fabric ensured the formation of phosphine oxide physical networks that are stable to 50 laundry cycles. Cellulose fabrics containing a minimum of 2 wt% phosphorus displayed excellent flame retardant behavior, characterized by LOI of $\geq$27.0% and after the flame time of 0 sec during the BKZ-VB Test. Based on the TGA-FTIR and DIP-MS analysis, a possible condensed (dominant) and gas (minor) mechanism of flame retardancy for the phosphine oxide polymers was proposed. The new treatment thus developed is not only efficient as a flame retardant but can be adapted to offer multifunctional treatments (i.e., antimicrobial functionality via incorporation of silver nanoparticles). Unlike other flame retardant treatments described in the literature, the new treatment ensures the treated fabric's excellent comfort. In the future, detailed investigations regarding the treatment of colored cellulose fabrics, impact on air permeability, cost evaluation, and optimization of other fabric properties will be performed, which will enable future commercialization of this technology.

Declaration of Competing Interest

The authors declare that they have no known competing financial interests or personal relationships that could have appeared to influence the work reported in this paper.

Acknowledgement

The authors acknowledge SNSF Grant IZSEZ0_182882 for partially funding this project. The NMR hardware was partially granted by the Swiss National Science Foundation (SNSF, Grant 206021_150638/1). The authors also acknowledge Zürcher Stiftung für Textilforschung (project number 116) for partially funding the project. The authors thank Mr. Silas Keller for the strength test of samples. We also thank Ms. Pierrine Zeller for whiteness index measurements and Ms. Patrizia Ballistreri for comfort measurements of the treated fabrics.

Appendix A. Supplementary data

NMR characterization, detailed synthesis procedure for Poly-A, Poly-B and cellulose treatment, Laundering of treated cellulose fabric, Cellulose digital pics after burning, MCC, TGA, TGA-FTIR, DIP-MS, EDX char, In-situ AgNP synthesis, and fabric appearance and comfort are given in supporting information. Supplementary data to this article can be found online at https://doi.org/10.1016/j.cej.2020.128028.

References

[1] S. Mandal, S. Annaheim, M. Camenzind, R.M. Rossi, Personal protective textiles and clothing, John Wiley & Sons, Inc., 2019, pp. 159-195.
[2] H. Yang, B. Yu, P. Song, C. Maluk, H. Wang, Surface-coating engineering for flame retardant flexible polyurethane foams: a critical review, Compos. Part B: Eng. 176 (2019).
[3] S.T. McKenna, N. Jones, G. Peck, K. Dickens, W. Pawelec, S. Oradei, S. Harris, A. A. Stec, T.R. Hull, Fire behaviour of modern facade materials – understanding the Grenfell Tower fire, J. Hazard. Mater. 368 (2019) 115–123.
[4] A.A. Stec, K. Dickens, J.L.J. Barnes, C. Bedford, Environmental contamination following the Grenfell Tower fire, Chemosphere 226 (2019) 576–586.
[5] J. Pickrell, Australian blazes will reframe our understanding of bushfire, Science (Washington, DC, U. S.), 366 (2019) 937.
[6] A. Gupta, S. Kumar, R. Kumar, A.K. Choudhary, K. Kumari, P. Singh, V. Kumar, COVID-19: emergence of infectious diseases, nanotechnology aspects, challenges, and future perspectives, ChemistrySelect, 5 (2020) 7521-7533.
[7] D.A. Holmes, A.R. Horrocks, Technical textiles for survival, Woodhead Publ. Ser. Text. 170 (2016) 287–323.
[8] O.A. El Seoud, M. Kostag, K. Jedvert, N.I. Malek, Cellulose regeneration and chemical recycling: closing the "cellulose gap" using environmentally benign solvents, Macromol. Mater. Eng. 305 (2020) 1900832.
[9] A.R. Horrocks, Flame retardant challenges for textiles and fibres: New chemistry versus innovatory solutions, Polym. Degrad. Stab. 96 (2011) 377–392.
[10] K.A. Salmeia, S. Gaan, G. Malucelli, Recent advances for flame retardancy of textiles based on phosphorus chemistry, Polymers 8 (2016) 319.
[11] D.V. Moiseev, B.R. James, Tetrakis(hydroxymethyl)phosphonium salts: Their properties, hazards and toxicities, Phosphorus Sulfur Silicon Relat. Elem. 195 (2020) 263–279.
[12] W. Wu, C.Q. Yang, Statistical analysis of the performance of the flame retardant finishing system consisting of a hydroxy-functional organophosphorus oligomer and the mixture of DMDHEU and melamine–formaldehyde resin, Polym. Degrad. Stab. 85 (2004) 623–632.
[13] W. Wu, C.Q. Yang, Comparison of different reactive organophosphorus flame retardant agents for cotton: Part I. The bonding of the flame retardant agents to cotton, Polym. Degrad. Stab. 91 (2006) 2541–2548.
[14] A. Duong, C. Steinmaus, C.M. McHale, C.P. Vaughan, L. Zhang, Reproductive and developmental toxicity of formaldehyde: a systematic review, Mutation Res./Rev. Mutation Res. 728 (2011) 118–138.
[15] Z. Chen, P. Xiao, J. Zhang, W. Tian, R. Jia, H. Nawaz, K. Jin, J. Zhang, A facile strategy to fabricate cellulose-based, flame-retardant, transparent and anti-dripping protective coatings, Chem. Eng. J. 379 (2020).
[16] W. Guo, X. Wang, J. Huang, Y. Zhou, W. Cai, J. Wang, L. Song, Y. Hu, Construction of durable flame-retardant and robust superhydrophobic coatings on cotton fabrics for water-oil separation application, Chem. Eng. J. 398 (2020).
[17] Y. Zhang, W. Tian, L. Liu, W. Cheng, W. Wang, K.M. Liew, B. Wang, Y. Hu, Eco-friendly flame retardant and electromagnetic interference shielding cotton fabrics with multi-layered coatings, Chem. Eng. J. 372 (2019) 1077–1090.
[18] F. Xu, L. Zhong, C. Zhang, P. Wang, F. Zhang, G. Zhang, Novel high-efficiency casein-based P-N-containing flame retardants with multiple reactive groups for cotton fabrics, ACS Sustainable Chem. Eng. 7 (2019) 13999–14008.
[19] S. Li, L. Zhong, S. Huang, D. Wang, F. Zhang, G. Zhang, A novel flame retardant with reactive ammonium phosphate groups and polymerizing ability for preparing durable flame retardant and stiff cotton fabric, Polym. Degrad. Stab. 164 (2019) 145–156.
[20] P. Tian, Y. Lu, D. Wang, G. Zhang, F. Zhang, Synthesis of a new N-P durable flame retardant for cotton fabrics, Polym. Degrad. Stab. 165 (2019) 220–228.
[21] C. Wan, G. Zhang, F. Zhang, A novel guanidine ammonium phosphate for preparation of a reactive durable flame retardant for cotton fabric, Cellulose 27 (2020) 3469–3483.
[22] S. Liu, C. Wan, Y. Chen, R. Chen, F. Zhang, G. Zhang, A novel high-molecular-weight flame retardant for cotton fabrics, Cellulose 27 (2020) 3501–3515.
[23] C. Wan, P. Tian, M. Liu, G. Zhang, F. Zhang, Synthesis of a phosphorus-nitrogen flame retardant endowing cotton with high whiteness and washability, Industrial Crops and Products 141 (2019).
[24] Z. Yang, X. Wang, D. Lei, B. Fei, J.H. Xin, A durable flame retardant for cellulosic fabrics, Polym. Degrad. Stab. 97 (2012) 2467–2472.
[25] Y. Jia, Y. Lu, G. Zhang, Y. Liang, F. Zhang, Facile synthesis of an eco-friendly nitrogen–phosphorus ammonium salt to enhance the durability and flame retardancy of cotton, J. Mater. Chem. A 5 (2017) 9970–9981.
[26] Y. Lu, Y. Jia, Y. Zhou, J. Zou, G. Zhang, F. Zhang, Straightforward one-step solvent-free synthesis of the flame retardant for cotton with excellent efficiency and durability, Carbohydrate Polymers 201 (2018) 438–445.
[27] D. Wang, L. Zhong, C. Zhang, S. Li, P. Tian, F. Zhang, G. Zhang, Eco-friendly synthesis of a highly efficient phosphorus flame retardant based on xylitol and application on cotton fabric, Cellulose 26 (2019) 2123–2138.
[28] S. Wang, X. Sui, Y. Li, J. Li, H. Xu, Y. Zhong, L. Zhang, Z. Mao, Durable flame retardant finishing of cotton fabrics with organosilicon functionalized cyclotriphosphazene, Polym. Degrad. Stab. 128 (2016) 22–28.
[29] L. Xu, W. Wang, D. Yu, Durable flame retardant finishing of cotton fabrics with halogen-free organophosphonate by UV photoinitiated thiol-ene click chemistry, Carbohydr. Polym. 172 (2017) 275–283.
[30] G. Rosace, C. Colleoni, V. Trovato, G. Iacono, G. Malucelli, Vinylphosphonic acid/methacrylamide system as a durable intumescent flame retardant for cotton fabric, Cellulose (Dordrecht, Neth.) 24 (2017) 3095–3108.
[31] J. Vasiljević, B. Tomšič, I. Jerman, B. Orel, G. Jakša, B. Simončič, Novel multifunctional water- and oil-repellent, antibacterial, and flame-retardant cellulose fibres created by the sol–gel process, Cellulose 21 (2014) 2611–2623.
[32] J.Y. Chen, L. Sun, W. Jiang, V.M. Lynch, Antimicrobial regenerated cellulose/nano-silver fiber without leaching, J. Bioact. Compat. Polym., 30 (2015) 17-33, 17 pp.
[33] M.A. Kebede, T. Imae, Sabrina, C.-M. Wu, K.-B. Cheng, Cellulose fibers functionalized by metal nanoparticles stabilized in dendrimer for formaldehyde decomposition and antimicrobial activity, Chem. Eng. J. (Amsterdam, Neth.), 311 (2017) 340-347.
[34] T. Pivec, S. Hribernik, M. Kolar, K.S. Kleinschek, Environmentally friendly procedure for in-situ coating of regenerated cellulose fibres with silver nanoparticles, Carbohydr. Polym. 163 (2017) 92–100.
[35] H.B. Ahmed, H.E. Emam, H.M. Mashaly, M. Rehan, Nanosilver leverage on reactive dyeing of cellulose fibers: color shading, color fastness and biocidal potentials, Carbohydrate Polym. 186 (2018) 310–320.
[36] C. Dong, L.-Y. Qian, G.-L. Zhao, B.-H. He, H.-N. Xiao, Preparation of antimicrobial cellulose fibers by grafting β-cyclodextrin and inclusion with antibiotics, Mater. Lett. 124 (2014) 181–183.
[37] M. He, H. Xiao, Y. Zhou, P. Lu, Synthesis, characterization and antimicrobial activities of water-soluble amphiphilic copolymers containing ciprofloxacin and quaternary ammonium salts, J. Mater. Chem. B 3 (2015) 3704–3713.
[38] M. He, Y. Zhou, H. Xiao, P. Lu, Amphiphilic cationic copolymers with ciprofloxacin: preparation and antimicrobial activities, New J. Chem. 40 (2016) 1354–1364.
[39] J. Miao, R.C. Pangule, E.E. Paskaleva, E.E. Hwang, R.S. Kane, R.J. Linhardt, J. S. Dordick, Lysostaphin-functionalized cellulose fibers with antistaphylococcal activity for wound healing applications, Biomaterials 32 (2011) 9557–9567.
[40] L. Fras-Zemljic, I. Kosalec, M. Munda, S. Strnad, M. Kolar, M. Bracic, O. Sauperl, Antimicrobial efficiency evaluation by monitoring potassium efflux for cellulose fibres functionalised by chitosan, Cellulose (Dordrecht Neth.) 22 (2015) 1933–1942.
[41] H. Li, L. Peng, Antimicrobial and antioxidant surface modification of cellulose fibers using layer-by-layer deposition of chitosan and lignosulfonates, Carbohydr. Polym. 124 (2015) 35–42.
[42] T. Ristic, S. Hribernik, L. Fras-Zemljic, Electrokinetic properties of fibers functionalized by chitosan and chitosan nanoparticles, Cellulose (Dordrecht, Neth.) 22 (2015) 3811–3823.
[43] T. Ristic, A. Zabret, L.F. Zemljic, Z. Persin, Chitosan nanoparticles as a potential drug delivery system attached to viscose cellulose fibers, Cellulose (Dordrecht, Neth.) 24 (2017) 739–753.
[44] Y.-A. Son, B.-S. Kim, K. Ravikumar, S.-G. Lee, Imparting durable antimicrobial properties to cotton fabrics using quaternary ammonium salts through 4-amino-benzenesulfonic acid–chloro–triazine adduct, Eur. Polymer J. 42 (2006) 3059–3067.
[45] S. Zhang, X. Yang, B. Tang, L. Yuan, K. Wang, X. Liu, X. Zhu, J. Li, Z. Ge, S. Chen, New insights into synergistic antimicrobial and antifouling cotton fabrics via dually finished with quaternary ammonium salt and zwitterionic sulfobetaine, Chem. Eng. J. 336 (2018) 123–132.
[46] S. Liu, H. Ye, Y. Zhou, J. He, Z. Jiang, J. Zhao, X. Huang, Study on flame-retardant mechanism of polycarbonate containing sulfonate-silsesquioxane-fluoro retardants by TGA and FTIR, Polym. Degrad. Stab. 91 (2006) 1808–1814.

[47] H.B. Kocer, I. Cerkez, S.D. Worley, R.M. Broughton, T.S. Huang, Polymeric antimicrobial N-halamine epoxides, ACS Appl. Mater. Interfaces 3 (2011) 2845–2850.
[48] G. Sun, X. Xu, J.R. Bickett, J.F. Williams, Durable and regenerable antibacterial finishing of fabrics with a new hydantoin derivative, Ind. Eng. Chem. Res. 40 (2001) 1016–1021.
[49] I. Sondi, B. Salopek-Sondi, Silver nanoparticles as antimicrobial agent: a case study on E. coli as a model for Gram-negative bacteria, J. Colloid Interface Sci. 275 (2004) 177–182.
[50] C. Keiser, C. Becker, R.M. Rossi, Moisture transport and absorption in multilayer protective clothing fabrics, Textile Res. J. 78 (2008) 604–613.
[51] R. Nazir, D. Parida, A.G. Guex, D. Rentsch, A. Zarei, A. Gooneie, K.A. Salmeia, K. M. Yar, F. Alihosseini, A. Sadeghpour, S. Gaan, Structurally tunable pH-responsive phosphine oxide based gels by facile synthesis strategy, ACS Appl. Mater. Interfaces 12 (2020) 7639–7649.
[52] P. Simonetti, R. Nazir, A. Gooneie, S. Lehner, M. Jovic, K.A. Salmeia, R. Hufenus, A. Rippl, J.-P. Kaiser, C. Hirsch, B. Rubi, S. Gaan, Michael addition in reactive extrusion: A facile sustainable route to developing phosphorus based flame retardant materials, Composites Part B: Engineering 178 (2019).
[53] W. Guo, Y. Hu, X. Wang, P. Zhang, L. Song, W. Xing, Exceptional flame-retardant cellulosic foams modified with phosphorus-hybridized graphene nanosheets, Cellulose 26 (2019) 1247–1260.
[54] S. Huo, S. Yang, J. Wang, J. Cheng, Q. Zhang, Y. Hu, G. Ding, Q. Zhang, P. Song, A liquid phosphorus-containing imidazole derivative as flame-retardant curing agent for epoxy resin with enhanced thermal latency, mechanical, and flame-retardant performances, J. Hazard. Mater. 386 (2020).
[55] S. Gaan, P. Rupper, V. Salimova, M. Heuberger, S. Rabe, F. Vogel, Thermal decomposition and burning behavior of cellulose treated with ethyl ester phosphoramidates: effect of alkyl substituent on nitrogen atom, Polym. Degrad. Stab. 94 (2009) 1125–1134.
[56] S. Gaan, G. Sun, Effect of phosphorus flame retardants on thermo-oxidative decomposition of cotton, Polym. Degrad. Stab. 92 (2007) 968–974.
[57] S. Gaan, G. Sun, K. Hutches, M.H. Engelhard, Effect of nitrogen additives on flame retardant action of tributyl phosphate: phosphorus–nitrogen synergism, Polym. Degrad. Stab. 93 (2008) 99–108.
[58] F.M. Uhl, G.F. Levchik, S.V. Levchik, C. Dick, J.J. Liggat, C.E. Snape, C.A. Wilkie, The thermal stability of cross-linked polymers: methyl methacrylate with divinylbenzene and styrene with dimethacrylates, Polym. Degrad. Stab. 71 (2001) 317–325.
[59] S.-L. Yang, Z.-H. Wu, W. Yang, M.-B. Yang, Thermal and mechanical properties of chemical crosslinked polylactide (PLA), Polymer Testing 27 (2008) 957–963.
[60] S. Gaan, G. Sun, Effect of nitrogen additives on thermal decomposition of cotton, J. Anal. Appl. Pyrolysis 84 (2009) 108–115.
[61] N. Li, J. Ming, R. Yuan, S. Fan, L. Liu, F. Li, X. Wang, J. Yu, D. Wu, Novel eco-friendly flame retardants based on nitrogen-silicone Schiff base and application in cellulose, ACS Sustainable Chem. Eng. 8 (2020) 290–301.
[62] H. Wu, R. Hu, B. Zeng, L. Yang, T. Chen, W. Zheng, X. Liu, W. Luo, L. Dai, Synthesis and application of aminophenyl-s-triazine derivatives as potential flame retardants in the modification of epoxy resins, RSC Adv. 8 (2018) 37631–37642.
[63] S. Yang, J. Wang, S. Huo, M. Wang, J. Wang, Preparation and flame retardancy of a compounded epoxy resin system composed of phosphorus/nitrogen-containing active compounds, Polym. Degrad. Stab. 121 (2015) 398–406.
[64] S. Huo, Z. Liu, J. Wang, Thermal properties and flame retardancy of an intumescent flame-retarded epoxy system containing phosphaphenanthrene, triazine-trione and piperidine, J. Thermal Anal. Calorimetry 139 (2020) 1099–1110.
[65] B.-G. Yao, Y. Li, J.-Y. Hu, Y.-L. Kwok, K.-W. Yeung, An improved test method for characterizing the dynamic liquid moisture transfer in porous polymeric materials, Polymer Testing 25 (2006) 677–689.
[66] M. Yatagai, S.H. Zeronian, Cellulose (London) 1 (1994) 205–214.
[67] P.J. Hauser, A.C. Gudac, Effects of alkaline treatments on physical and dyeing properties of cotton woven fabrics, AATCC Rev. 8 (2008) 45–48.
[68] M. Yamamoto, Y. Kashiwagi, M. Nakamoto, Size-controlled synthesis of monodispersed silver nanoparticles capped by long-chain alkyl carboxylates from silver carboxylate and tertiary amine, Langmuir 22 (2006) 8581–8586.
[69] J.D.S. Newman, G.J. Blanchard, Formation of gold nanoparticles using amine reducing agents, Langmuir 22 (2006) 5882–5887.
[70] S. Sirohi, A. Mittal, R. Nain, N. Jain, R. Singh, S. Dobhal, B. Pani, D. Parida, Effect of nanoparticle shape on the conductivity of Ag nanoparticle poly(vinyl alcohol) composite films, Polymer Int. 68 (2019) 1961–1967.
[71] H.D. Beyene, A.A. Werkneh, H.K. Bezabh, T.G. Ambaye, Synthesis paradigm and applications of silver nanoparticles (AgNPs), a review, Sustainable Mater. Technol. 13 (2017) 18–23.
[72] S. Ravindra, Y. Murali Mohan, N. Narayana Reddy, K. Mohana Raju, Fabrication of antibacterial cotton fibres loaded with silver nanoparticles via "Green Approach", Colloids Surfaces A: Physicochem. Eng. Aspects 367 (2010) 31–40.
[73] T.G. Volova, A.A. Shumilova, I.P. Shidlovskiy, E.D. Nikolaeva, A.G. Sukovatiy, A. D. Vasiliev, E.I. Shishatskaya, Antibacterial properties of films of cellulose composites with silver nanoparticles and antibiotics, Polymer Testing 65 (2018) 54–68.
[74] D. Parida, P. Simonetti, R. Frison, E. Bülbül, S. Altenried, Y. Arroyo, Z. Balogh-Michels, W. Caseri, Q. Ren, R. Hufenus, S. Gaan, Polymer-assisted in-situ thermal reduction of silver precursors: a solventless route for silver nanoparticles-polymer composites, Chem. Eng. J. 389 (2020).
[75] A.V. Fuchs, S. Ritz, S. Pütz, V. Mailänder, K. Landfester, U. Ziener, Bioinspired phosphorylcholine containing polymer films with silver nanoparticles combining antifouling and antibacterial properties, Biomater. Sci. 1 (2013) 470–477.